

Perturbation method for the dynamic analysis of a bistable oscillator under slow harmonic excitation

Angelo Luongo^{*1}, Sara Casciati^{2a} and Daniele Zulli^{1b}

¹*M&MoCS, International Research Center on Mathematics and Mechanics of Complex Systems, University of L'Aquila, Via Giovanni Gronchi, 18, 67100 L'Aquila (AQ), Italy*

²*DICAr-Dipartimento di Ingegneria Civile e Architettura, University of Catania, Italy*

(Received September 26, 2015, Revised April 21, 2016, Accepted May 6, 2016)

Abstract. In this paper a nonlinear, bistable, single degree of freedom system is considered. It consists of a Duffing oscillator externally excited by a non-resonant, harmonic force. A customized perturbation scheme is proposed to achieve an approximate expression for periodic solutions. It is based on the evaluation of the quasi-steady (slow) solution, and then on a variable change followed by two perturbation steps which aim to capture the fast, decaying contribution of the response. The reconstructed solution, given by the sum of the slow and fast contributions, is in a good agreement with the one obtained by numerical integration.

Keywords: energy harvesting; duffing oscillator; slow-fast dynamics; perturbation method

1. Introduction

The dynamical response of the bi-stable oscillators under slow harmonic excitation is separated into two distinct components, related to the low and high frequencies (slow and fast oscillations), respectively, where the slow variable modulates the fast one, giving rise to the specific phenomenon of bursting. This feature recently became of great interest for energy harvesting purposes, since it can be exploited to extend the harvester efficiency to situations where the ambient vibrational energy is distributed over a wide spectrum and dominant at low frequencies (below resonance).

A review of different analytical techniques as well as experiments dealing with bistable systems is given in Harne and Wang (2013). A multi-scale perturbation scheme is proposed in Amin Karami and Inman (2011) for an electro-mechanical harvesting device with both quadratic and cubic nonlinear terms; there, the Authors limit their perturbation analysis just to describe intra-well oscillations whereas, on the other hand, inter-well oscillations have been considered in the framework of numerical techniques, as it is pointed out in the review paper by Harne and Wang (2013) too. In Han (2011), the possibility of triggering the bursting in bistable oscillators is described. The analysis of this phenomenon which is typical in dynamical systems with singular

*Corresponding author, Professor, E-mail: angelo.luongo@univaq.it

^a Associate Professor, E-mail: sacasci@unict.it

^b Assistant Professor, E-mail: daniele.zulli@univaq.it

perturbation (see Verhulst (2005), Verhulst (2007)) is carried out in Kovacic and Cartmell (2014) for a large class of oscillators. An evaluation of the beneficial contribution of a hardening nonlinear stiffness in devices suitable to harvesting purposes can be found in Ramlan *et al.* (2010). Furthermore, a general decomposition method for dynamical systems characterized by slow-fast transitions is given in Blackman (2004).

The exploitation of nonlinear phenomena in a bistable plate for energy harvesting purpose is carried out in Arrieta *et al.* (2010), while super-harmonic frequency bands of a nonlinear twin-well oscillator are analyzed in Masana *et al.* (2012) for harvesting energy from low-frequency excitations. A ferromagnetic cantilever converter coupled to an external magnet under random vibrations is analyzed in Ferrari *et al.* (2010) and Ferrari *et al.* (2011) to produce electric energy using piezoelectric effect, comparing numerical simulations to experimental tests. Simulations on a nonlinear piezomagnetoelastic energy harvester driven by stationary Gaussian white noise under stochastic resonance are carried out in Litak (2010). The coupling of a piezoelectric cantilever to a static magnetic field to enhance energy harvesting performance is studied in Lin *et al.* (2010), broadband random ambient vibrations exciting a piezomagnetoelastic energy harvesters are considered in Ali (2011).

In many studies, the dynamic analysis of bistable oscillators starts from a piecewise linear approximation of the restrain force, as in Cohen *et al.* (2012). Analytical techniques are often pursued in order to gain an insight when searching the solution, as proposed in Pilipchuk (2009) and Uspensky and Avramov (2014) for the case of free vibrations, and in Shaw and Holmes (1983) and Zou and Nagarajaiah (2015) for the cases in which the external forcing terms are present. As a matter of fact, the solutions describe rich classes of motions, as shown in Cao *et al.* (2008) and Cao *et al.* (2008), where numerical and semi-analytical methods, like Melnikov theory, are applied to a harmonically forced piecewise linear oscillator in order to derive the bifurcation diagrams and detect the chaotic attractors. In Cohen *et al.* (2012) and Cohen and Bucher (2014), the decomposition of the solution of an energy harvesting bistable oscillator in its slow and fast components is performed, and the analysis of the single terms is carried out guided by the experimental results.

In this paper a nonlinear, bistable, single degree of freedom system, as the one studied in Cohen *et al.* (2012) and Cohen and Bucher (2014), is considered. It is subjected to a slow base motion such that the operational conditions are far below resonance, and it is described by a Duffing oscillator under a slow external excitation. The system periodic solution is modelled by the superimposition of a slow part, describing the inter-well evolution, and a fast, decaying, contribution which is triggered after each jump inside the potential well. Based on these assumptions, a customized perturbation scheme is proposed to obtain an analytical, approximated solution able to describe such periodic motions.

The paper is organized as follows: In Section 2, a brief description of the physical model is given, and the equation of motion is presented. In Section 3, the perturbation scheme is described and then, in Section 4, some numerical results are shown for comparison. Finally, the conclusions are drawn in Section 5.

2. The model

The possibility of developing a customized perturbation approach able to derive an approximate analytical expression of the response of a bistable oscillator under harmonic

excitation is investigated with reference to a harvesting device found in the literature Cohen *et al.* (2012), Cohen and Bucher (2014). The scheme of the device is shown in Fig. 1 and it consists of a rigid frame supporting an oscillator of mass m , with a linear spring and a damper of coefficients k and c , respectively. Moreover, the mass is constrained by a nonlinear tool which provides a potential barrier; it is actually realized by two opposing magnets. The frame is subjected to a (slow) harmonic base motion of frequency σ , and the relative motion between the mass and the frame induces a voltage in a static coil. In this paper, the transduction mechanism used for energy harvesting is not considered, with the focus being placed on the customization of a perturbation method suitable to derive an approximate expression for the periodic solutions of the bistable oscillator.

Let $z(t)$ denote the normalized displacement of the mass, where t is the time. The nondimensional equation of motion governing the dynamics of the bistable oscillator is

$$\ddot{z} + 2\xi\omega\dot{z} + f(z) = -F \cos(\sigma t + \varphi) \tag{1}$$

where

$$f(z) = -\bar{c}_1 z + c_3 z^3 \tag{2}$$

with $\bar{c}_1, c_3 > 0$. A qualitative plot of $f(z)$ is shown in blue line in Fig. 2. In Eq. (1), the dot denotes the time-derivative, ζ is the damping factor, F the amplitude of the excitation and φ the initial phase. Its autonomous version shows three equilibria: $z_0 \equiv 0$, which is unstable, and $z_{1,2} \equiv \pm \sqrt{\frac{\bar{c}_1}{c_3}}$, which are stable. The linearized problem around one of the two non-trivial equilibria has natural frequency $\omega = \sqrt{f'(z_{1,2})} = \sqrt{2\bar{c}_1}$, which is typically much greater than σ (the prime indicates differentiation with respect to z). Therefore Eq. (1) describes a Duffing oscillator subjected to a slow, non-resonant, external excitation.

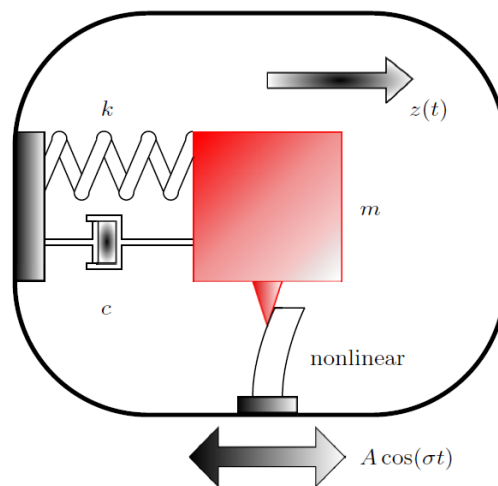


Fig. 1 Scheme of the energy harvesting device

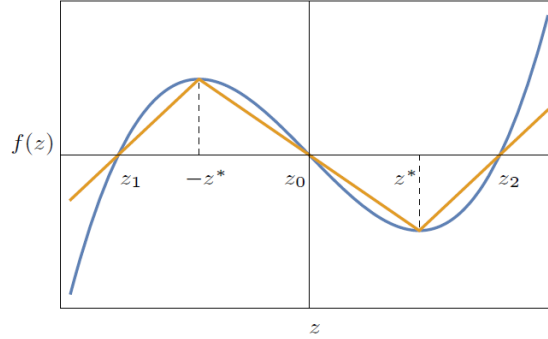


Fig. 2 Nonlinear response function $f(z)$ (blue) and tri-linear approximation $g(z)$ (orange)

3. The perturbation scheme

The existence of periodic solutions of Eq. (1) is discussed in Cohen and Bucher (2014). It is shown that, in the case of a sufficiently high amplitude of the excitation F , they are typically characterized by a slow-frequency oscillating component, representing the inter-well excursions, superimposed to a fast-frequency decaying oscillation, representing the intra-well motion, which is triggered after each inter-well jump. Both the components have amplitudes of the same order of magnitude. Here, a perturbation scheme is proposed, with the aim of obtaining an approximate expression for periodic motions. Based on the above described features of the solutions, one pursues a method able to represent the different contributions at successive perturbation steps.

First, a rescaling of the time variable is performed by defining a slow time-scale $\tau := \sigma t$, which implies that $\frac{d}{dt} = \sigma \frac{d}{d\tau}$, $\frac{d^2}{dt^2} = \sigma^2 \frac{d^2}{d\tau^2}$, with σ a small parameter. Eq. (1) is then written in terms of the rescaled time:

$$\sigma^2 \ddot{z} + 2\xi \omega \dot{z} + f(z) = -F \cos(\tau + \varphi) \quad (3)$$

having indicated by a dot, from now on, the differentiation with respect to τ . The presence of the small parameter σ as a factor of the higher order derivatives in Eq. (3) shows the nature of a singular perturbation Verhulst (2005), Verhulst (2007). Accordingly, for most of the time, the solution of Eq. (3) is ruled by the quasi-steady component (no inertia, nor damping involved). On the other hand, when approaching the jumps, which occur when the solution reaches the folds of the response function, the first and second order derivatives of $z(t)$ become larger, thus making the inertial and damping terms in Eq. (3) of the same order of magnitude as the elastic term. These considerations suggest (1) to evaluate the quasi-steady component, which results significant in the construction of the overall solution, and, (2) to express the motion as the sum of the quasi-steady and dynamic parts.

3.1 Quasi-steady solution

By posing $\sigma=0$ in Eq. (3), the following nonlinear algebraic equation is obtained

$$f(z(\tau)) = -F \cos(\tau + \varphi) \quad (4)$$

in which τ is a parameter that governs the quasi-steady response. To simplify its evaluation, the response function is written as

$$f(z) = g(z) + \varepsilon(f(z) - g(z)) \tag{5}$$

where $\varepsilon > 0$ is a small bookkeeping parameter. The function $g(z)$ is defined as

$$g(z) = \begin{cases} \bar{\omega}^2(z + \bar{z}), & z < -z^* \\ -r^2 z, & -z^* \leq z \leq z^* \\ \bar{\omega}^2(z - \bar{z}), & z > z^* \end{cases} \tag{6}$$

and it represents the chosen tri-linear approximation of the cubic expression of $f(z)$. The parameters $\bar{\omega}, r, \bar{z}, z^*$ which define the tri-linear approximation are assigned as follows:

$\bar{z} := |z_{1,2}|$, $z^* := \pm \sqrt{\frac{\bar{c}_1}{3c_3}}$ (so that $f(z^*)=0$), $\bar{\omega} := \sqrt{\frac{|f(z^*)|}{|z_2| - z^*}}$ and $r = \sqrt{|f'(0)|}$. These assumptions

lead to a tri-linear approximation $g(z)$ as the one qualitatively shown in Fig. 2 by an orange line, superimposed to the cubic restrain force $f(z)$.

Eq. (5) means that $f(z)$ is written as the tri-linear approximation plus the (small) difference between the exact and the tri-linear approximation; actually, to avoid ordering violation, this difference has to be kept small.

At the leading order $\varepsilon=0$, Eq. (4) is replaced by

$$g(z(\tau)) = -F \cos(\tau + \varphi) \tag{7}$$

and its solution is evaluated as

$$v_0 = -\frac{F}{\bar{\omega}^2} \cos(\tau + \varphi) - \bar{z} \psi(\tau), \quad \tau \in [0, 2\pi] \tag{8}$$

where $\psi(\tau) = H(\tau) - 2H(\tau - \pi)$ and $H(\tau)$ is the Heaviside step.

The first addend in Eq. (8) is the smooth part of the solution, describing the evolution of the system into the potential well, namely along the stable part of the tri-linear curve; the second addend, which is non-smooth, is responsible for the inter-well jumps, supposed as instantaneous and occurring at $\tau=0, \pi, 2\pi$. These contributions, as well as the complete $v_0(\tau)$, are shown in Fig. 3(a). The phase plot for $v_0(\tau)$ is given in Fig. 3(b). In Fig. 3(c) the function $g(v_0)$ is superimposed to the tri-linear response function $g(z)$. Sudden jumps between the two branches of the solution correspond to horizontal lines in Fig. 3b,c. They occur when the solution reaches the sharp corner of the response function, where instability is triggered (orange dotted line in Fig. 3(c)). On the other hand, for most of the time, the solution lies on the stable branches, meaning that the mass executes oscillations around one of the two equilibria.

It is worth noticing that Eq. (4) is a cubic nonhomogeneous equation, whose solution can be obtained by using Cardano formula; it provides the exact expression of the quasi-static contribution, which could substitute the expression of $v_0(\tau)$ given in Eq. (7) and obtained by the tri-linear approximation of the response function. However, such an exact solution suffers from the drawback of being multivalued, where jumps occur in correspondence of the turning points. This

peculiarity would make the further implementation of the perturbation method much more difficult, therefore, in the following calculations it is chosen to use the approximation given by Eq. (7). For the sake of completeness, the obtained exact contribution is shown in Fig. 3a in dash-dotted (red) line.

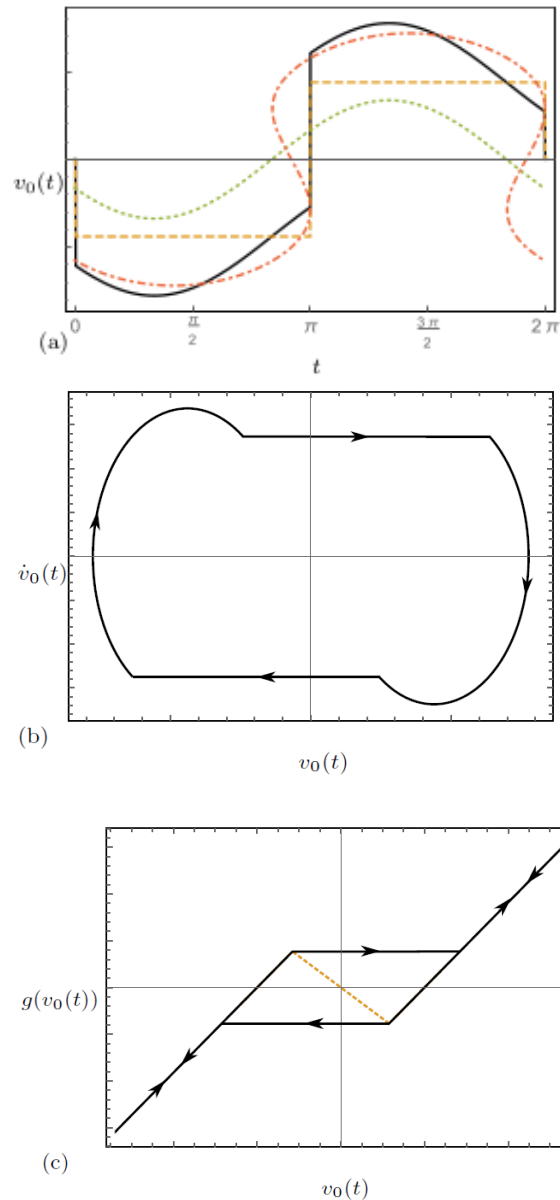


Fig. 3 Qualitative plots of the quasi-steady solution over one period: (a) time evolution of the quasi-steady solution (black continuous line), its smooth component (green dotted line) and its non-smooth component (orange dashed line), superimposed to the exact, multivalued, solution of Eq. (4) (red dash-dotted line), (b) phase plot and (c) response function (black continuous line) superimposed to the tri-linear function (orange dotted line)

3.2 Dynamic contribution

The solution of Eq. (3) is expressed by superimposing an unknown dynamic contribution $u(\tau)$ to the quasi-steady solution $v_0(\tau)$, so that one reads

$$z(\tau) = v_0(\tau) + u(\tau) \tag{9}$$

where the dynamic contribution is assumed to be of the same order of magnitude of the steady one. Eq. (9) should be meant as a change of variable. The unknown dynamic term is expanded as

$$u(\tau) = u_0(\tau) + \varepsilon u_1(\tau) \tag{10}$$

By substituting Eqs. (5), (9) and (10) in Eq. (3) and collecting and vanishing the terms multiplying ε^0 and ε^1 , the following perturbation equations are obtained

$$\begin{aligned} \varepsilon^0 : \quad & \sigma^2 \ddot{u}_0 + 2\xi \omega \sigma \dot{u}_0 + g(v_0) + \bar{\omega}^2 u_0 = \\ & -F \cos(\tau + \varphi) - \sigma^2 \ddot{v}_0 - 2\xi \omega \sigma \dot{v}_0 \\ \varepsilon^1 : \quad & \sigma^2 \ddot{u}_1 + 2\xi \omega \sigma \dot{u}_1 + \bar{\omega}^2 u_1 = \\ & -(f(v_0 + u_0) - g(v_0 + u_0)) \end{aligned} \tag{11}$$

Moreover, after using Eq. (8) as solution of Eq. (7), Eq. (11a) becomes

$$\sigma^2 \ddot{u}_0 + 2\xi \omega \sigma \dot{u}_0 + \bar{\omega}^2 u_0 = -\sigma^2 \ddot{v}_0 - 2\xi \omega \sigma \dot{v}_0 \tag{12}$$

As a consequence of the tri-linear shape of $g(z)$, the non-smooth part is shifted to the right-hand side of both Eqs. (12) and (11). It is worth noticing that the ε -order dynamic correction $u_1(\tau)$, which is given by the solution of Eq. (11b), takes into account the difference between the nonlinear and tri-linear response functions.

The solvability condition has to be imposed at each perturbation step: it requires that the solutions are 2π -periodic, i.e.

$$\begin{aligned} u_j(0) &= u_j(2\pi) \\ \dot{u}_j(0) &= \dot{u}_j(2\pi) \end{aligned} \tag{13}$$

for $j=0,1$.

The solution of Eq. (12) is obtained after replacing the non-smooth part inside $v_0(\tau)$, namely $\psi(\tau)$, with its (smooth) truncated Fourier expansion

$$\psi(\tau) \cong \frac{4}{\pi} \sum_{n=1}^N \frac{\sin[(2n-1)\tau]}{2n-1} \tag{14}$$

In particular, it turns out to be

$$\begin{aligned}
u_0(\tau) &= e^{-\xi \frac{\omega}{\sigma} \tau} (a_0 \cos(\lambda \tau) + b_0 \sin(\lambda \tau)) \\
&+ \frac{F \sigma \left((\sigma^2 + 4\xi^2 \omega^2 - \bar{\omega}^2) \cos(\tau + \varphi) - 2\xi \omega \bar{\omega}^2 \sin(\tau + \varphi) \right)}{\bar{\omega}^2 (\sigma^4 + \bar{\omega}^4 + \sigma^2 (4\xi^2 \omega^2 - 2\bar{\omega}^2))} \\
&+ \bar{z} \sigma \frac{4}{\pi} \sum_{n=1}^N \frac{a_n \cos[(2n-1)\tau] + b_n \sin[(2n-1)\tau]}{k_n}
\end{aligned} \tag{15}$$

where

$$\begin{aligned}
\lambda &= \frac{\bar{\omega}}{\sigma} \sqrt{1 - \xi^2 \frac{\omega^2}{\bar{\omega}^2}} \\
a_n &= -2\xi \omega \bar{\omega}^2 \\
b_n &= \sigma(2n-1) \left(\sigma^2(2n-1)^2 + 4\xi^2 \omega^2 - \bar{\omega}^2 \right) \\
k_n &= \left((1-2n)^2 \sigma^2 - \bar{\omega}^2 + 2\xi \omega \left(\xi \omega - \sqrt{\xi^2 \omega^2 - \bar{\omega}^2} \right) \right) \times \\
&\quad \left((1-2n)^2 \sigma^2 - \bar{\omega}^2 + 2\xi \omega \left(\xi \omega + \sqrt{\xi^2 \omega^2 - \bar{\omega}^2} \right) \right)
\end{aligned} \tag{16}$$

and a_0, b_0 can be found by substituting Eq. (15) to Eq. (13) for $j=0$.

As a final step, the perturbation Eq. (11) can be analytically solved for $u_1(\tau)$, after using Eqs. (8), (14), (15) and applying the solvability condition (13) for $j=1$. Unfortunately, its expression is cumbersome and it is omitted here for the sake of brevity.

4. Numerical results

The considered case study is characterized by the following values of the parameters in Eqs. (1) and (2): $\bar{c}_1=0.5$, $c_3=0.125$, $\omega=1$, $\xi=0.07$, $\varphi=0.4$. The function $f(z)$ is shown in Fig. 4(a), and its potential $U(z)=\int f(z)dz$ in Fig. 4(b). In this case, the two non-trivial equilibria are $z_{1,2}=\pm 2$. Note that the natural frequency of the linearized problem around one of the two non-trivial equilibria is $\omega=1$.

The value $\sigma=0.1$ is assigned, meaning that one assumes an external excitation with a frequency ten times smaller than the natural frequency of the linearized problem.

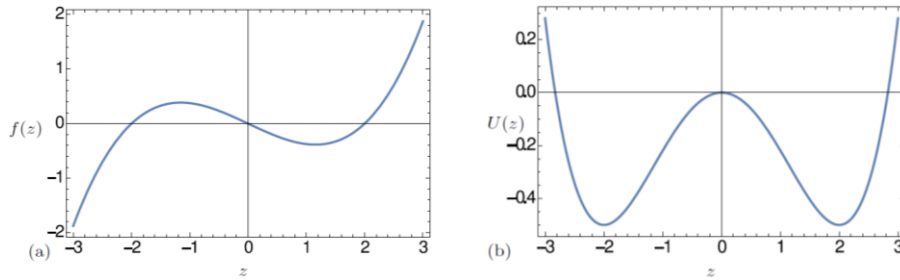


Fig. 4 Nonlinear response function: a) force; b) potential

The numerical integration of Eq. (1) shows a 2π -periodic evolution (see Fig. 5) for $F=1.535$, whereas a quasi-periodic solution appears for some different values of F (see Fig. 6 for $F=0.614$). Here, the attention is focused only on the periodic solutions. Therefore, from now on, only the value $F=1.535$ is considered. From the power spectrum in Fig. 5(c), it is evident that components of frequency higher than $\Omega=1$ are involved in the solution.

A first choice (case I) of the tri-linear approximation is shown by an orange line in Fig. 7. As a consequence of this choice, the solution $z(\tau)$ obtained after solving Eq. (12), namely $z(\tau)=v_0(\tau)+u_0(\tau)$ is shown in Fig. 8 by a red line, and is superimposed to the numerical solution of the original Eq. (3). The number of Fourier terms in the expansion of $\psi(\tau)$ is $N=6$, which is checked to be large enough to guarantee the convergence. A bad agreement between the two obtained time-functions is obtained, thus suggesting that the ε -order correction, $u_1(\tau)$, will not be able to cover the gap between them. On the other hand, as a positive note, the higher frequency contributions are induced in the solution, as evident in Fig. 8(c), although they do not show a satisfactory agreement from a quantitative point of view.

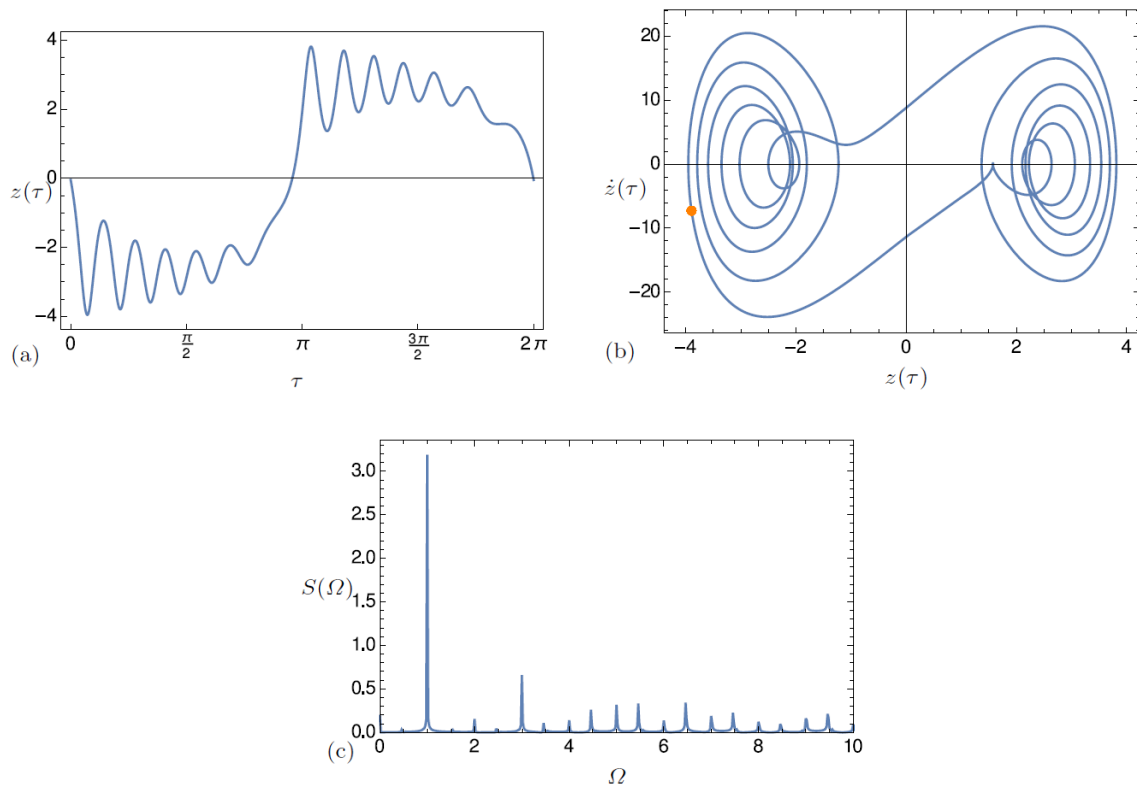


Fig. 5 Numerical integration for $F=1.535$: (a) 2π -periodic evolution of $z(\tau)$ and (b) phase plot with superimposed Poincaré map (orange point), (c) power spectrum $S(\Omega)$

Therefore, a different tri-linear approximation is considered (case II), as shown in Fig. 7 in red line. It is evaluated using a least squares procedure, in order to minimize the difference $f(z)-g(z)$ along the stable branches. In this case, the solution of Eq. (12) provides a better agreement for $z(\tau)$, as shown in Fig. 9. On the other hand, this last case provides a worst approximation of $f(z)$ in the neighbourhood of the turning point, suggesting that the choice of the tri-linear approximation is ultimately related to the amplitude level F of the system excitation. In particular, for high level of F , as the one which is considered in this example, the system evolution covers large part of the lateral, stable, branches in Fig. 7, therefore it is plausible that the approximation of the $f(z)$ through the red line is a good choice in order to describe the dynamics of the system. However, for lower levels of F (provided that they trigger inter-well excitations), where covering of the stable branches by the system evolution is limited, the first choice of tri-linear approximation, namely the orange curve in Fig. 7, turns out to be the good enough.

As a final step, still for case II, the solution of Eq. (11) is used to reconstruct the complete solution $z(\tau)=v_0(\tau)+u_0(\tau)+\varepsilon u_1(\tau)$, which is shown by a black line in Fig. 10. It shows a satisfactory agreement with the numerical results from both the qualitative and quantitative points of view.

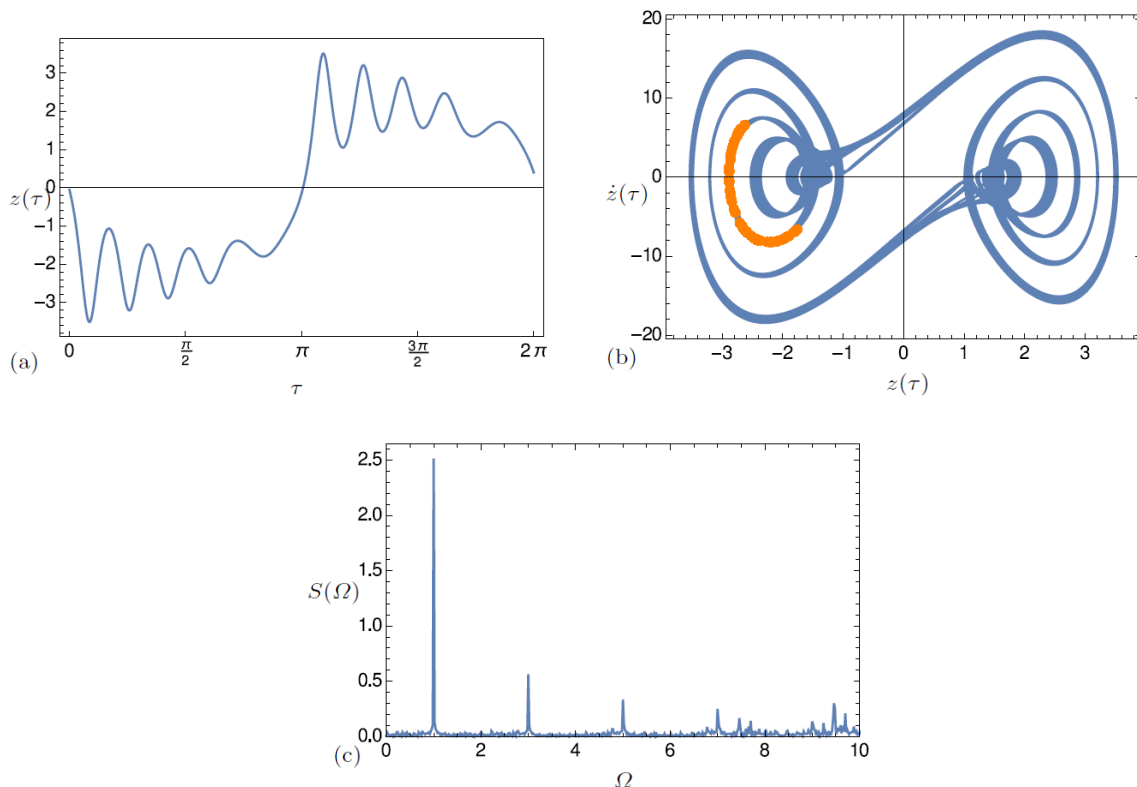


Fig. 6 Numerical integration for $F=0.614$: (a) quasi-periodic evolution of $z(\tau)$ and (b) phase plot with superimposed Poincaré map (orange point), (c) power spectrum $S(\Omega)$

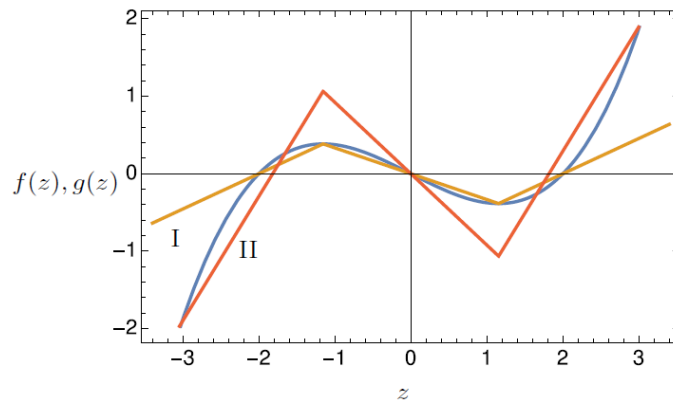


Fig. 7 Response function (blue line) and tri-linear approximations (case I: orange line, case II: red line)

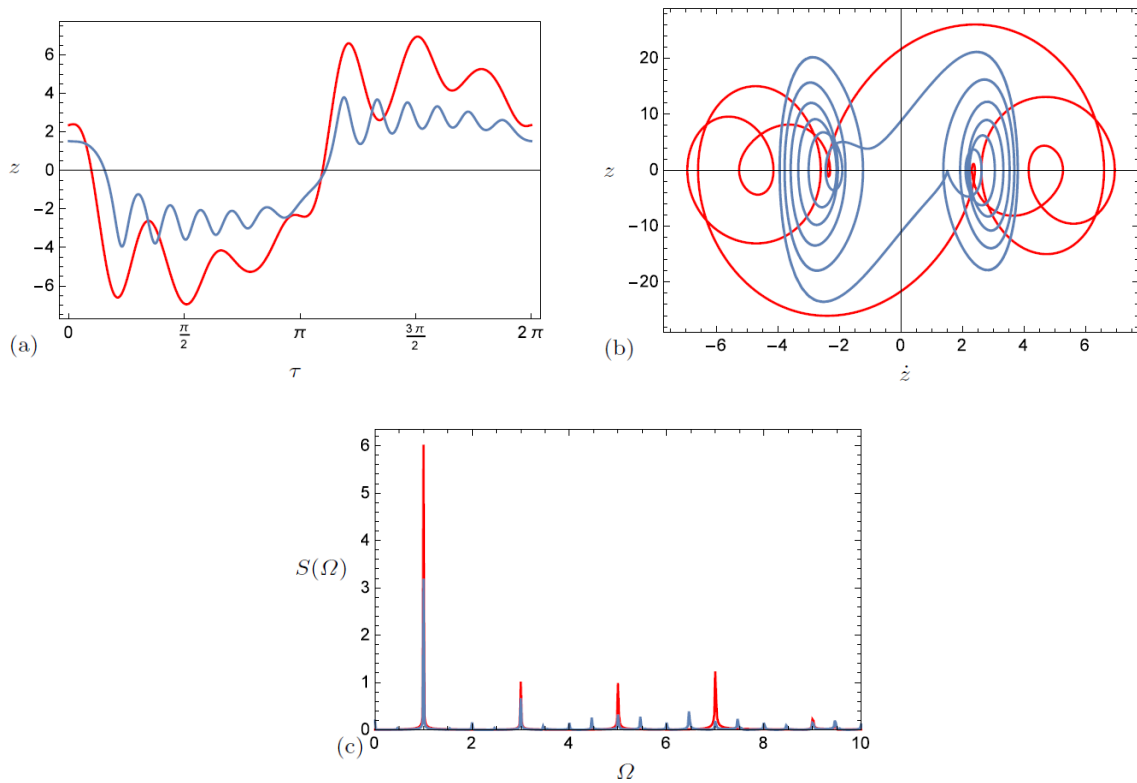


Fig. 8 First order response $z(\tau)=v_0(\tau)+u_0(\tau)$ evaluated using tri-linear function I (red lines): (a) time evolution in one period, (b) phase plot and (c) power spectrum. Blue line: numerical solution of the original equation

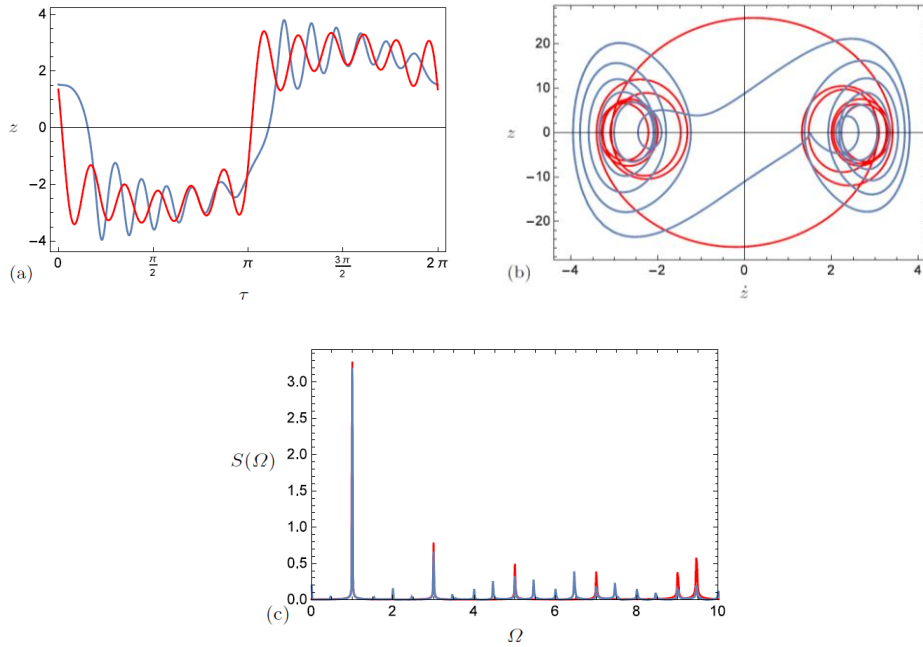


Fig. 9 First order response $z(\tau)=v_0(\tau)+u_0(\tau)$ evaluated using tri-linear function II (red lines): (a) time evolution in one period, (b) phase plot and (c) power spectrum. Blue line: numerical solution of the original equation

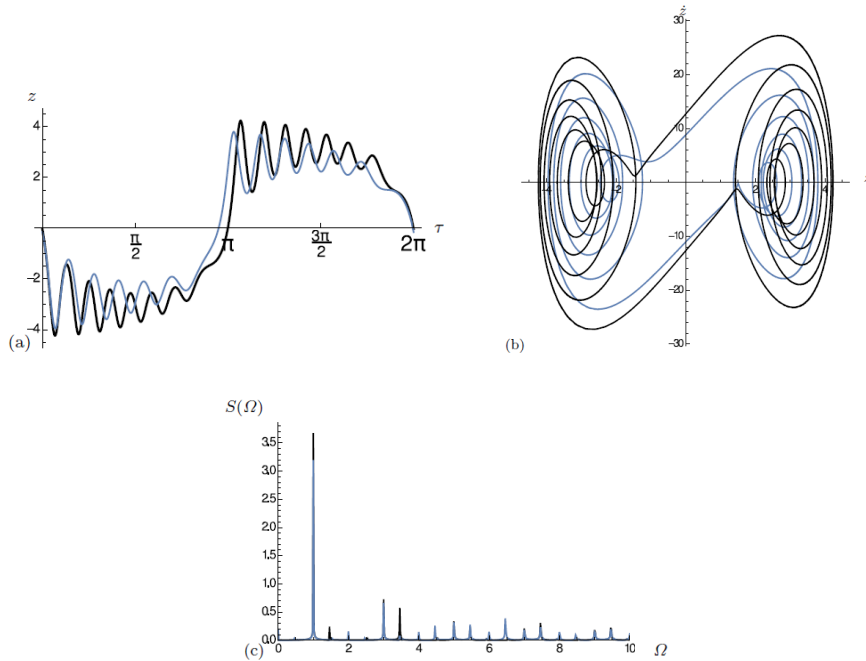


Fig. 10 Second order response $z(\tau)=v_0(\tau)+u_0(\tau)+\epsilon u_1(\tau)$ evaluated using tri-linear function II (black lines): (a) time evolution in one period and (b) phase plot and (c) power spectrum. Blue line: numerical solution of the original equation

5. Conclusions

In this paper a nonlinear, bistable, single degree of freedom system is considered. It consists of a Duffing oscillator under a slow, non-resonant external force. After a qualitative discussion of the solution, a customized perturbation method is proposed. It relies on the evaluation of the quasi-steady component for a tri-linear approximation of the cubic response function. The quasi-steady component contains both smooth and non-smooth contributions, with the first one expressing the slow evolution of the mass, and the last one describing the sudden jumps occurring between the two potential wells. Moreover, after a variable change, a dynamic contribution to the solution is introduced and expanded in series. It describes the fast decaying oscillations which are re-induced after each jump. The reconstructed solution, sum of the slow and fast contributions, is in good agreement with the one obtained by numerical integrations.

The proposed perturbation steps, drawn after a mechanical interpretation of the components of the solution, offer the possibility of easily obtaining an approximated analytical expression for it, reproducing, in case of periodicity, the main aspects of the numerical one. As a counterpart, the good quantitative agreement relies on a good choice of an underlying tri-linear approximation $g(z)$ of the exact cubic response function $f(z)$, requesting that the difference between them should be kept small in the range of definition of the oscillations, which depends on the amplitude of the external force.

Acknowledgments

The research described in this paper was financially supported by the Natural Science Foundation.

References

- Ali, S.F., Adhikari, S., Friswell, M.I. and Narayanan, S. (2011), "The analysis of piezomagnetoelastic energy harvesters under broadband random excitations", *J. Appl. Phys.*, **109**(7), 074904.
- Amin Karami, M. and Inman, J. (2011), "Equivalent damping and frequency change for linear and nonlinear hybrid vibrational energy harvesting systems", *J. Sound Vib.*, **330** (23), 5583-5597.
- Arrieta, A.F., Hagedorn, P., Erturk, A. and Inman, D.J. (2010), "A piezoelectric bistable plate for nonlinear broadband energy harvesting", *Appl. Physics Lett.*, **97**, 104102.
- Blackman, I. (Ed.) (2004), *Selected topics in vibrational mechanics*, World Scientific Publishing, New Jersey.
- Cao, Q., Wiercigroch, M., Pavlovskaja, E., Thompson, J.T. and Grebogi, C. (2008a), "Piecewise linear approach to an archetypal oscillator for smooth and discontinuous dynamics", *Philos. T. R. Soc. A*, **366**, 635-652.
- Cao, Q., Wiercigroch, M., Pavlovskaja, E.E., Grebogi, C. and Thompson, J.T. (2008b), "The limit case response of the archetypal oscillator for smooth and discontinuous dynamics", *Int. J. Nonlinear Mech.*, **43** (6), 462-473.
- Cohen, N. and Bucher, I. (2014), "On the dynamics and optimization of a non-smooth bistable oscillator - Application to energy harvesting", *J. Sound Vib.*, **333**, 4653-4667.
- Cohen, N., Bucher, I. and Feldman, M. (2012), "Slow-fast response decomposition of a bi-stable energy harvester", *Mech. Syst. Signal Pr.*, **31**, 29-39.
- Ferrari, M. Baù, M. Guizzetti, M. and Ferrari, V. (2011), "A single-magnet nonlinear piezoelectric converter

- for enhanced energy harvesting from random vibrations”, *Sensor. Actuat. A: Phys.*, **172**(1),287-292.
- Ferrari, M., Ferrari, V., Guizzetti, M., Andò, B., Baglio, S. and Trigona, C. (2010), “Improved energy harvesting from wideband vibrations by nonlinear piezoelectric converters”, *Sensor. Actuat. A: Phys.*, **162**(2), 425-431.
- Han, Q. and Bi, X. (2011), “Bursting oscillations in duffing’s equation with slowly changing external forcing”, *Commun Nonlinear Sci Numer Simulat.*, **16**, 4146-4152.
- Harne, R.L. and Wang, K.W. (2013), “A review of the recent research on vibration energy harvesting via bistable systems”, *Smart Mater. Struct.*, **22** (2), 023001.
- Kovacic, I. and Cartmell, M. (2014), “On the behaviour of bistable oscillators with slowly varying external excitation”, *ENOC Proceedings*, Wien, July.
- Lin, J.T., Lee, B. and Alphenaar, B. (2010), “The magnetic coupling of a piezoelectric cantilever for enhanced energy harvesting efficiency”, *Smart Mater. Struct.*, **19**(4), 045012.
- Litak, G., Friswell, M.I. and Adhikari, S. (2010), “Magnetopiezoelectric energy harvesting driven by random excitations”, *Appl. Phys. Lett.*, **96**(21), 214103.
- Masana, R. and Daqaq, M.F. (2012), “Energy harvesting in the super-harmonic frequency region of a twin-well oscillator”, *J. Appl. Phys.*, **111**, 044501.
- Pilipchuk, V.N. (2009), “Closed-form periodic solutions for piecewise-linear vibrating systems”, *Nonlinear Dynam.*, **50**, 169-178.
- Ramlan, R., Brennan, M.J., Mace, B.R. and Kovacic, I. (2010), “Potential benefits of a non-linear stiffness in an energy harvesting device”, *Nonlinear Dynam.*, **59**, 545-580.
- Shaw, S.W. and Holmes, P.J. (1983), “A periodically forced piecewise linear oscillator”, *J. Sound Vib.*, **90** (1), 129-155.
- Uspensky, B. and Avramov, K. (2014), “Nonlinear modes of piecewise linear systems under the action of periodic excitation”, *Nonlinear Dynam.*, **76**(2), 1151-1156,
- Verhulst, F. (2005), *Methods and Applications of Singular Perturbations*. Springer-Verlag, Berlin.
- Verhulst, F. (2007), “Singular perturbation methods for slow-fast dynamics”, *Nonlinear Dynam.*, **50** (4), 747–753, ISSN 0924-090X. 10.1007/s11071-007-9236-z.
- Zou, K. and Nagarajaiah, S. (2015), “Study of a piecewise linear dynamic system with negative and positive stiffness”, *Commun Nonlinear Sci Numer Simulat.*, **22**, 1084-1101.